SHUAIBA TRANSITION ZONE FIELDS: FROM LABORATORY SCAL EXPERIMENTS TO FIELD DEVELOPMENT CHALLENGES

I. Abu-Shiekah[(1)], S.K. Masalmeh[(2)] and X.D. Jing[(2)]
(1) Petroleum Development Oman (PDO)
(2) Shell Technology Oman (STO)

This paper was prepared for presentation at the International Symposium of the Society of Core Analyst held in Abu Dhabi, UAE 29 October -2 November, 2008

ABSTRACT

The field production data from the Shuaiba formation in Oman demonstrate the potential of recovering oil from the capillary transition zones. However, due to the uncertainties in characterizing the initial oil saturation distribution and describing the oil mobility and residual oil saturation through the transition zone, accurate prediction of oil production and ultimate recovery from these transition zones especially for the fields with relatively thin oil columns (~5-30m) but large areal extents remain an ongoing challenge. To address this challenge, in the past ten years extensive core characterization and special core analysis (SCAL) experimental data have been gathered from the Shuaiba formation. These SCAL data together with geological, petrophysical and field dynamic data have led to an improved prediction of waterflooding performance from such transition zone fields.

This paper addresses the issue of reducing uncertainty in determining the distribution of the initial oil saturation in the heterogeneous low-relief Shuaiba capillary transition zones. An extensive SCAL programme consisting of mercury air capillary pressure curves, electrical resistivity index and relative permeability/imbibition capillary pressure measurements under representative reservoir conditions from the Shuaiba fields have been conducted in the past 10 years. The capillary pressure data are influenced by the geological heterogeneity at different scales and therefore special efforts in analyses and upscaling are needed to reconcile the capillary pressure data with saturation logs. The measured values of the Archie saturation exponent show a range of variations from 2-4 across the different fields as a result of varying pore size distributions and wettability. The range of initial saturation uncertainties and its impact on establishing proper saturation height functions and subsequently the STOIIP distributions for selected transition zone field cases will be discussed. Finally this paper will show examples of predicted well performances from different parts of the fields compared against the actual production data. The results highlight the generic trends in transition zone oil production and the recommended procedures of static and dynamic modeling during field development planning.

INTRODUCTION

Shuaiba formation contains a significant portion of Oman's hydrocarbon volumes. A subset that consists of a cluster of six fields with more than two billion barrels of initial oil in place (STOIIP) is the subject of this paper. A sizable part of the STOIIP of these fields is

located in the transition zone. The fields in question have different levels of reservoir and fluid complexities. Some of the reservoirs are matrix dominated and have low oil viscosities (1- 5 cP). Other fields are heavily fractured and the oil viscosity is in the range of 8-500 cP. Three of the fields in question are being developed through horizontal oil producers and injectors flooding patterns. Other naturally fractured reservoirs with heavier oil are designated for EOR development after primary depletion. Irrespective of the development options, initial oil distribution in the transition zone is equally important for both water flooding optimization and EOR options.

The permeability of the Shuaiba formation for most of the oil bearing sections is in the range of 1-10 mD, while the porosity is in the range of 15-40%. Several fields have a top thin layer of favourable reservoir properties (permeability in excess of 10 mD and relatively high initial oil saturation). However detailed characterization of this layer is problematic due to frequent core damage hence the difficulty of capturing enough core plugs from such a reservoir section.

One common feature of these fields is that most of the initial oil in place is in the capillary transition zone, often with low oil saturation in low-dipping structures spreading over extensive areas. In some cases the oil bearing sections of the reservoir can be as thin as 5 m and the maximum attainable initial oil saturation at the top of the reservoir is in the range of 60-70%. The water phase with a saturation of 30-40% at the structure top is mobile since the measured irreducible water saturation can be as low as 5%. Figure 1 shows the reservoir structure and the initial oil saturation distribution in one of the transition zone fields. The amount of recoverable oil in a transition zone depends on the distribution of initial oil saturation (Soi) as a function of depth, as well as the general relative permeability and capillary pressure characteristics including the Sor/Soi relationship.

The majority of the wells in these fields are single or multi-lateral horizontal oil producers completed in the transition zone. Therefore, variable relative permeability and imbibition capillary pressure curves as a function of initial oil saturation, are vital to capture reservoir performance for both water flooding and EOR projects (Masalmeh et al., 2007). Horizontal wells offer an opportunity for improved oil recovery from tight formations if they are placed at the optimal depth and avoiding injector/producer short-cuts via fractures or high permeability streaks. For the Shuaiba transition zones, horizontal wells have their planning, operational and modeling challenges (Vij et al., 1998). One such challenge is to locate the horizontal wells at the highest initial oil saturation range along their total trajectory which in the case of Shuaiba reservoirs extends to about 2000 m net horizontal reservoir sections. The key enablers to achieve this objective are to have both properly characterized initial saturation height functions for well planning and geosteering tools for necessary trajectory corrections.

In this paper SCAL data from different fields are used for initial oil saturation distribution modeling. Cores of several hundred meters are available from different wells in the fields under study. CT scanning was conducted on whole core and plugs to exam sample heterogeneity in order to select suitable samples for SCAL experiments. Due to the strong

variations of rock/fluid properties, mercury injection capillary pressure in addition to the basic porosity and permeability measurements are the common data available from all concerned fields. Other more advanced measurements such as electrical properties, oil water capillary pressure and relative permeability curves are less frequent, especially for the relatively heavy oil fields.

SPECIAL CORE ANALYSIS

Primary Drainage Capillary Pressure

Primary drainage capillary pressure measurements were conducted using mercury injection, centrifuge and porous plate techniques. Mercury injection capillary pressure (MICP) measurements were performed on a large number of samples from the different fields because it is fast, cheap, and it is not affected by insufficient cleaning (Masalmeh and Jing, 2006). The capillary pressure curves are mostly measured on end trims and in some cases on larger pieces cut from plug samples. Figure 2 shows mercury-air capillary pressure curves measured on samples from one of the fields under study. The measurements show strong variations of entry capillary pressures. The spread of capillary pressure curves shown in this figure represents the range of measured MICP curves with permeability range of 1-10 mD from the fields.

There is a general trend where the capillary entry pressure increases with decreasing permeability. However, it is difficult to find a unique correlation between the plug permeability and the measured Pc on the trim end mainly due to the heterogeneity of the core material which makes the trim ends not always representative of the plug samples. We have investigated this effect by comparing mercury-air Pc curves measured on two or more pieces taken from the same 1.5 " plug or measured on two different trim ends from twin plugs. An example of Pc curves measured on four twin samples taken within a 8 cm interval is shown in Figure 3. The porosity and permeability of the four 1.5" diameter "twin" plugs are in the range of 26-27% and 1.9-2.4 md, respectively. CT scans and NMR T2 measurements were carried out on the plug samples to assess sample heterogeneity and suitability for further tests. The variation in the capillary entry pressure cannot be explained by the variation of permeability and porosity. This variation in capillary pressure is due to the heterogeneity in the core material and an up-scaled capillary pressure would represent this permeability range. The up-scaled capillary pressure curve for any given reservoir unit is calculated using the procedure described in (Ekrann 1999; Abu-Shiekah et. al. 2007):

$$S_w^{upscaled}(P_c) = \frac{\sum_{j=1}^{n} S_{wj}(P_c) * \varphi_j * V_j}{\sum_{j=1}^{n} \varphi_j * V_j} \quad \text{...}(1)$$

The up-scaled Pc for the selected interval is also shown in Figure 3. The corresponding relative permeability curves were also measured on the plugs and relative permeability

upscaling for this type of hetergenoeous carbonates under waterflooding follows the procedure by Abu-Shiekah et al. (2007).

Centrifuge capillary pressure measurements were conducted using crude oil for fields that have relatively low viscous oil at reservoir temperature. In some cases matching of the capillary pressure curves with those of mercury air is not achieved due to the heterogeneity of the plugs as mentioned above or due to potential ineffective cleaning. Porous plate equilibrium method measurements are limited due to high oil viscosity and low permeability plugs. However, for homogeneous plugs a good match was observed between the MICP and both the centrifuge and the porous-plate equilibrium method.

Measurements of Electrical Resistivity Index

For electrical log interpretation, both formation factor and saturation exponents were measured. Figure 4 shows the formation factors from different Shuaiba fields at representative reservoir stress conditions. The cementation exponent has a mean value of $m=1.9 \pm 0.1$.

The saturation exponent measurements were conducted using dead crude oil following either the continuous injection (de Waal et al., 1989) or the equilibrium porous plate methods at reservoir temperatures. The saturation exponent ranges from n=2 up to n=4 (Table 1). The measured saturation exponents show a wider range of variations than the cementation exponents. Relatively high values of saturation exponents were seen more in the heavily fractured Shuaiba heavy oil reservoirs classified as "oil wet" fields due to the effects of wettability and pore geometries (as explained in Jing et al., 1993, Fleury, 2002).

Measurements of Fluid Properties

In addition to the standard PVT sampling, measurement and analysis, fluid properties such as water resistivity, fluid density and interfacial tension are needed for proper saturation height functions modeling. The crude oil viscosity plays a significant role in determining the type of laboratory measurements due to its direct impact on equilibration time for capillary pressure measurements and impact on cleaning efficiency.

Water properties are characterized by high salinity brine (150,000 ppm – 210,000 ppm) and hence low water resistivity at reservoir temperature. The measured interfacial tension between the synthetic formation brine and reservoir dead crude oil from the different fields shows a range up to 30 mN/m. The crude oil viscosity covers a range as shown in Table 1.

Dynamic SCAL – Bounding/Scanning Relative Permeability and Capillary Pressure

For proper dynamic modeling of transition zone, we need to incorporate the residual oil saturation (Sor)/initial oil saturation (Soi) relationship and apply relative permeability and capillary pressure models that are calibrated against experimental data and honour the correct physical characteristics of the capillary transition zone. In addition to the S_{or}/S_{oi} relationship, relative permeability of oil and water, as well as imbibition capillary pressure curves starting at different initial oil saturations (relative permeability scanning curves), are also needed for transition-zone reservoir simulation. Using one relative permeability curve

that starts at connate water (bounding curve) to characterize the entire transition zone will underestimate the oil mobility in such reservoirs. A SCAL program has been carried out to generate the necessary relative permeability and capillary pressure data required fro transition zone modeling. A procedure of deriving imbibition capillary pressure from drainage capillary pressure for oil-wet carbonates taking into account SCAL calibration was applied (Masalmeh and Jing, 2006).

To illustrate how the relative permeability and capillary pressure models work, the water and oil relative permeability and the capillary pressure bounding and scanning curves generated using the model published earlier (Masalmeh et. al. 2007) are shown in Figure 5**.** This model has been used in the current study, after calibration using the SCAL data measured on rock samples from the Shuaiba reservoirs.

SATURATION HEIGHT FUNCTION MODELING

The fields under study are developed mainly using horizontal wells of up to 2000 m long. In some of the wells the hydrocarbon column thickness is lower than 10 m which is comparable to the uncertainty range in the true vertical depth measurement for horizontal wells. Prior knowledge about the saturation height functions with reasonable range of uncertainty is essential input to define the well trajectory and the target depth. However, long horizontal wells are subject to true vertical depth uncertainty and are more exposed to lateral formation heterogeneities. For instance, a change of 100 psi mercury injection drainage Pc corresponds to 10-30 meters (depending on the fluid properties) difference in the height above free water level and which is of comparable size to the reservoir thickness. The other challenge is that the resistivity logs at high salinity and relatively high temperature are less sensitive to high water saturation if lateral logs are used instead of induction logs (Schlumberger, 1991).

Coring such horizontal wells is uncommon and often the number of cored vertical wells or pilot holes is not sufficient to constrain lateral heterogeneity. This necessitates the need to make the most out of any data available to constrain reservoir description and hydrocarbon distribution. Reconciliation of available SCAL data with fluid and saturation logs is vital to achieve predictive saturation height function, necessary to populate geological models with the right initial oil saturation. Initial oil saturation distribution in transition zone fields is essential to predict reservoir performance, especially for reservoirs that are thin and low dipping and where sizable part of the STOIIP is located in the capillary transition zone.

To estimate initial hydrocarbon distribution in the fields, resistivity logs are interpreted using measured mean cementation and saturation exponents, e.g., Field A in Table 1. A capillary pressure model was derived based on the data shown in Figure 2. The field consist of two main layers in the Shuaiba formation where each is sub-divided to one or more sub-layers. The top main layer has variable thickness of few meters and it has more favourable properties (both permeability and oil saturation). The bottom layer and its sub-layers are tight and have a thick transition zone. Two different capillary pressure curves have been used to initialize the static model, one for the top layer and the other is for the bottom layer. The two capillary pressure curves are obtained by up-scaling the data shown

in Figure 2 from each layer using equation (1), one for the top layer and the other for the bottom layer. In the up-scaling process each curve was given the same rock volume fraction. A good match was obtained between the log and the Pc derived saturation data. A selection of synthetic logs for both horizontal and vertical wells is shown in Figure 6.

DYNAMIC WELL/FIELD PERFORMANCE

Wells in the transition zone regardless of the average initial oil saturation are producing oil and water at the same time from the start of the well life. The ratio of water to oil production from each well segment is dependent on initial water saturation and directly related to the mobility ratio between water and oil:

$$M = \frac{K_{rw}(S_{wi}, S_w)}{\mu_w} \Big/ \frac{K_{ro}(S_{wi}, S_w)}{\mu_o} \quad \text{.....(2)}$$

High oil recovery is associated with a large amount of water production. In a previous publication (Masalmeh et. al. 2007) we presented mechanistic modeling that focused on the key factors that control production performance from a transition zone. We also showed that transition zone may produce almost dry oil, and in other cases, it may cut significant water from day one, depending on the initial oil saturation, heterogeneity, relative permeability, and capillary pressure hysteresis. The transition-zone model and methodology presented in the pervious publication were used in this study. Relative permeability and capillary pressure scanning curves have been generated at different initial oil saturations. The relative permeability and capillary pressure models with the bounding and scanning curves and Sor/Soi relations described earlier have been implemented in a simulation model using the Shell in-house reservoir simulator (MoReS). These models have been used in history matching field data, both oil and water production and reservoir pressure. To compare with conventional approach of modeling transition zone, we have performed runs using relative permeability bounding curves alone. In the next paragraphs actual field data and full field simulations in support of the previous findings will be presented.

Laboratory SCAL measurements from one medium size field (A) showed that the residual oil saturation of the bounding curves is in the ranges of 20-25%. The average maximum initial oil at the top of the reservoir is about 60%, while the overall field estimated average oil saturation is about 40%. This transition-zone field produced to date more than 27% of the total oil in place through water flooding development. Figure 7 shows both the water cut from individual wells as well as from the total field as a function of cumulative produced oil. Although some of the produced water is due to water channelling or high permeability streaks, the majority of water is due to the mobile water in the capillary transition zone. As shown in the figure almost all the wells started producing water from day 1. Note that for some wells most of the water is produced at water cut of more than 90%. This demonstrates that to achieve high oil recovery from transition zone, high water production needs to be tolerated.

A second field (B) is of a smaller size than the above field (A). Dynamic laboratory experiments showed similar residual oil and relative permeability trends. The initial oil saturation extends to about 90% at the top of the reservoir as shown in Figure 1 and Figure 6a and 6b. Field development is by horizontal wells following the structure to the flank where oil saturation decreases when approaching the oil water contact. The overall recovery factor to date is about 35%. The upscaled geological model together with the saturation height functions described above and the measured relative permeability curves are used to construct a dynamic model. Historical total oil and water production from the field are matched without any tuning of the geological model using the measured scanning relative permeability curves. Improved matching for the individual well performance requires some slight adjustment of properties in the geological model which is within geological uncertainty for this type of settings. In all geological realizations saturation height functions and scanning relative permeability models were kept the same. In each case using the bounding relative permeability models without the scanning curves tends to underestimate oil production and overestimate water production. Figure 8 shows both the water cut from individual wells as well as from the total field as a function of cumulative produced oil. As shown in the figure a close match was achieved for the different wells and the overall field data. One of the crestal wells (crestal well B) produced more than 9 million barrels of oil, with water production only started 8 years after oil production due to the high initial oil saturation. Other flank wells where oil saturation decreases with depth, started producing water from day one, as shown in Figure 8.

Water production from such fields is attributed to both mobile formation water associated with oil production and channelled water production from injectors (fractures/high perm streaks) and aquifers (coning). To achieve high oil recovery factors requires optimizing the well trajectory in relatively uniform initial oil saturation sections to avoid the dominance of water production from high initial water saturation sections. The flank well B in Figure 8 has low oil saturation at the toe just 10 meters above the water injection well.

Figures 9 and 10 take a closer look at the data of two wells. Figure 9 shows the measured down hole pressure (Fig. 9a) and water rate and oil rate (Fig. 9b) as a function of time for crestal well B. The well is located at the top of the structure and it has high initial oil saturation. The figure shows both field data and the history match from two different runs. The first run was performed using proper transition zone modelling incorporating relative permeability scanning curves (SC) and the second run was performed using bounding curves (BC) alone. The figure shows a good history match when using scanning curves, but the match was lost when using bounding curves alone. Figure 10 shows the water and oil production rate as a function of time for a flank well which has low initial oil saturation. The well started producing water from day 1. Similar to the previous well, a good history match was obtained when using scanning curves while the history match was lost when using bounding curves alone.

These two wells shown in Figures 9-10 illustrate the importance of including proper modeling of transition zone by including scanning curves. The behavior of crestal well B (Fig. 9) shows in the first eight years when the oil production was coming mainly from the

high oil saturation part, both relative permeability models (scanning curves or bounding curves alone) could match the field data. In this case the scanning curves at low initial oil saturation have no impact and oil mobility is well described by the bounding curve. However, as water production starts, the bounding curve model could not history match the data. Here oil and water are coming from lower part of the structure where the mobility of the oil is strongly dependent on initial oil saturation and can only be captured by relative permeability scanning curves. For the second well (Fig. 10), the bounding curve model failed to history match the data from day 1 as the well was completed in the part of the structure where both oil and water are mobile.

In summary, these Shuaiba transition zone fields have average oil saturation less than 50% and most of the STOIIP may be located in the bottom of the transition zone depending on the height of the oil column. Developing such fields requires careful characterisation and accurate modelling of initial oil saturation vs. height and the necessary dynamic multi-phase flow properties following the scanning oil relative permeability and imbibition PC curves as described by Masalmeh et al. (2007). The field performances have been correctly predicted using the transition zone modelling procedure calibrated with laboratory and field data.

CONCLUSIONS

1. The understanding and prediction of transition-zone oil recovery need to start from an accurate static model to characterize the geological heterogeneities and petrophysical properties that influence the initial saturation distributions. Saturation-height functions derived from logs and drainage capillary pressure curves should be reconciled to accurately calculate initial saturation distributions through the transition zones.
2. To achieve high oil recovery factors from transition zones requires optimizing the well trajectory in relatively high initial oil saturation sections to avoid the dominance of water production from high initial water saturation sections.
3. Close agreement has been obtained between simulation-model predictions and actual well/field production performances, demonstrating the benefits of improved characterization and modeling of capillary transition zones in significantly reducing uncertainties and aiding field-development planning.
4. Special Core Analysis plays a key role in accurate modeling of initial oil saturation distribution and subsequent prediction of waterflood performance of Shuaiba transition zone reservoirs.

ACKNOWLEDGEMENTS

We thank the Ministry of Oil & Gas of Oman for granting permission to publish this paper. We also would like to thank our colleagues in Petroleum Development Oman (PDO) and Shell Technology Oman (STO) for stimulating discussions and support.

REFERENCES

1. Abu Shiekah, I., Masalmeh, S.K. and Jing, X.D.: “Experimental Investigation and Modelling of Waterflooding Performance of a Bioturbated Carbonate Formation”, SCA-19 presented at the SCA 2007 conference, Calgary, Canada, 10-12 September, (2007).
2. De Waal J.A., Smits, R.M.M, de Graaf, J.D. and Schipper, B.A.: "Measurement and Evaluation of Resistivity-Index Curves", The Log Analyst, SPWLA Thirtieth Annual Logging Symposium, June 11-14, 1989.
3. Ekrann, S.: "Water Saturation Modeling: An Upscaling Point of View". SPE 56559, paper presented at SPE Annual Technical Conference and Exhibition in Houston, Texas, 3-6 October 1999.
4. Fleury M.:” Resistivity in Carbonates: New Insights”, SPE 77719, paper presented at the SPE Annual Technical Conference and Exhibition, San Antonio, Texas, 29 September-2 October, 2002.
5. Jing, X.D, Gillespie, A and Trewin, B.M.: “Resistivity Index From Non-Equilibrium Measurements Using Detailed In-Situ Saturation Monitoring”, SPE 26798, paper presented at the Offshore European Conference held in Aberdeen, September 7-10, 1993.
6. Masalmeh, S.K., Jing, X.D.: “Carbonate SCAL: Characterization of Carbonate Rock Types for Determination of Saturation Functions and Residual Oil Saturation”, SCA-08 presented at the SCA 2004 conference, Abu Dhabi, October (2004).
7. Masalmeh, S.K. and Jing, X.D: “Capillary Pressure Characteristics of Carbonate Reservoirs: Relationship between Drainage and Imbibition Curves”. SCA2006-16, in Proceedings of the International Symposium of the Society of Core Analysts Trondheim, Norway, 12-16 September, (2006).
8. Masalmeh, S.K., Abu Shiekah, I. and Jing, X.D.: "Improved Characterization and Modeling of Capillary Transition Zones in Carbonate Reservoirs". SPE paper 109094, SPE Reservoir Evaluation & Engineering, Vol. 10 (2): 191-204 APR (2007).
9. Schlumberger: "Log Interpretation Principles/Applications", 1991.
10. Vij, S.K., Narasaiah, S.L., Walia, Anup and Singh, Gyan: "Multilaterals: An Overview and Issues Involved in Adopting This Technology". SPE- 39509-MS, paper presented at SPE India Oil and Gas Conference and Exhibition, 17-19 February 1998, New Delhi, India.

Table 1: Saturation exponents of different fields from Shuaiba.

Field	Dead Crude Oil Viscosity at Reservoir Temperature	Brine Salinity (ppm)	Saturation Exponent <n>
A	~2	151000	1.8-2.0
B	3.0-3.5	210000	2.0-2.5
C	~6	154000	2.0-2.2
D	~16	170000	3.0-4
E	~25	213000	2.0-2.5
F	>1000	NA	NA

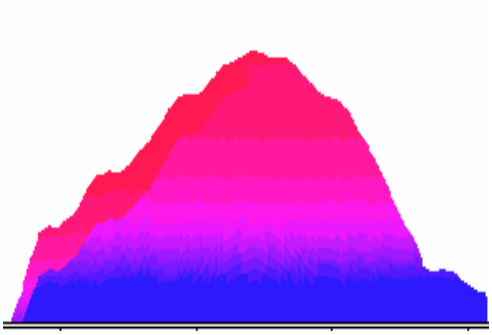

Figure 1: A cross-section of oil saturation vs. depth map of a transition zone field.

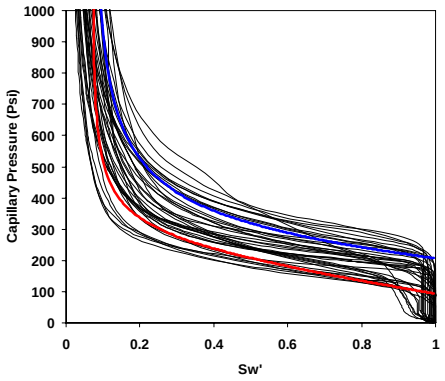

Figure 2: Mercury injection capillary pressure curves and two up-scaled capillary pressure curves to match saturation logs (thick blue line on top for the tighter layer, thick red line at bottom for the more permeable layer).

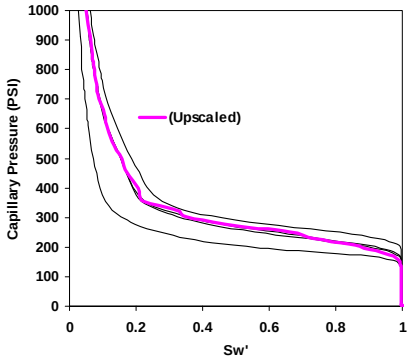

Figure 3: Measured mercury injection drainage capillary pressure curves from four trim ends (thin lines) and an up-scaled curve (thick line) assuming each of the four trim has the same volume fraction.

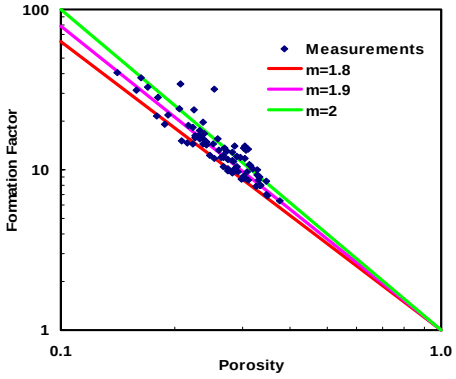

Figure 4: Measured formation factor of 79 plugs from different fields of Shuaiba formation.

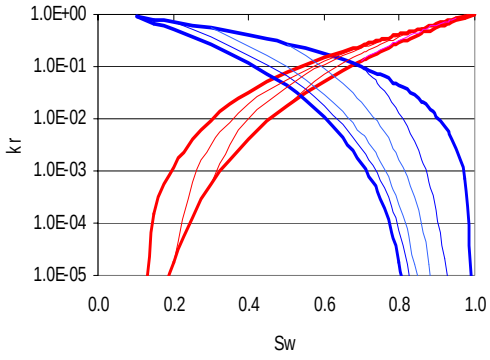

Figure 5a: Oil and water relative permeability bounding (thick lines) and scanning curves (thin lines), after Masalmeh et. al. 2007.

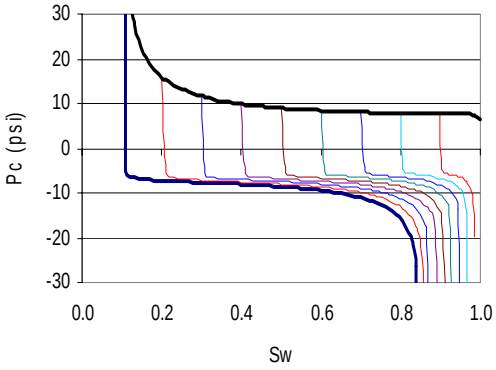

Figure 5b: Capillary pressure bounding (thick lines) and imbibition scanning curves (thin lines), after Masalmeh et. al. 2007.

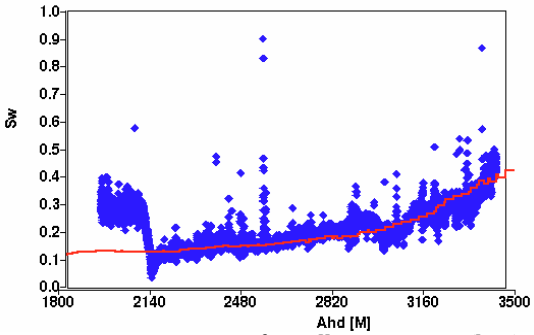

Figure 6a: Comparison of capillary pressure (line) and log based (symbols) saturation height functions from a horizontal well.

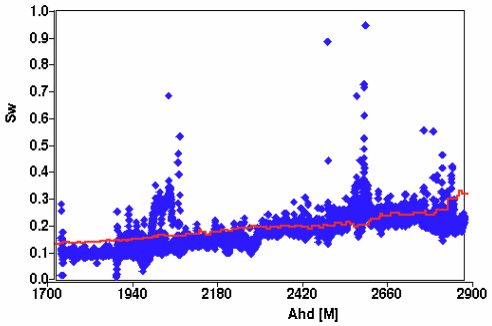

Figure 6b: Comparison of capillary pressure (line) and log based (symbols) saturation height functions from a horizontal well.

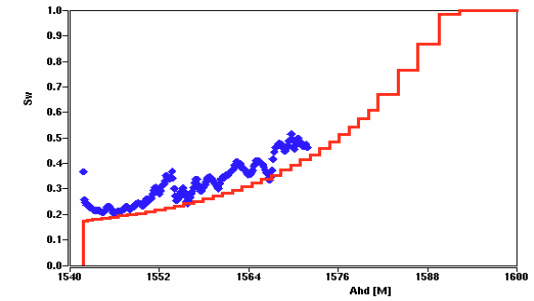

Figure 6c: Comparison of capillary pressure (line) and log based (symbols) saturation height functions from a vertical well.

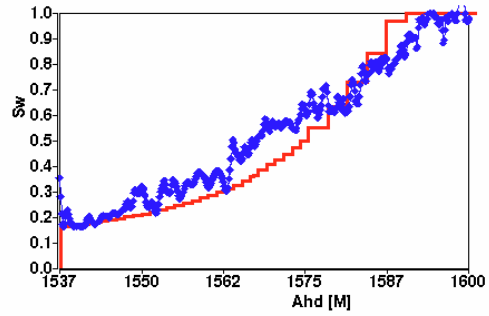

Figure 6d: Comparison of capillary pressure (line) and log based (symbols) saturation height functions from a vertical well.

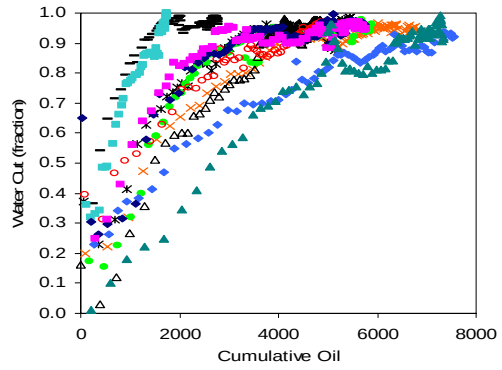

Figure 7a: Water cut as a function of the cumulative oil produced of selected transition zone wells.

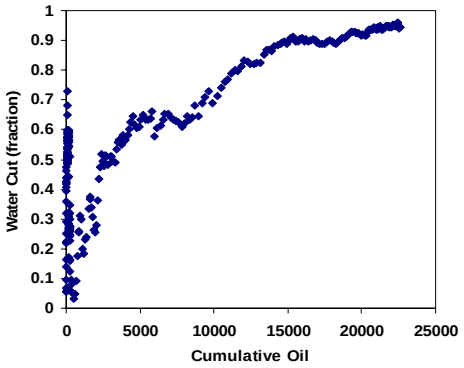

Figure 7b: Water cut as a function of the cumulative oil produced of the total transition zone field.

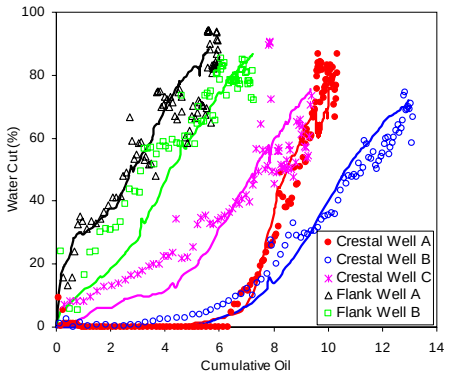

Figure 8a: Water and oil production from crestal and flank wells. The figure shows both field data (symbols) and simulation history match (lines).

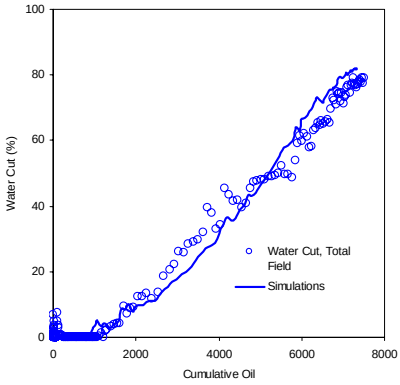

Figure 8b: Water cut of the field as a function of cumulative oil. The figure shows both field data (symbols) and simulation history match (line).

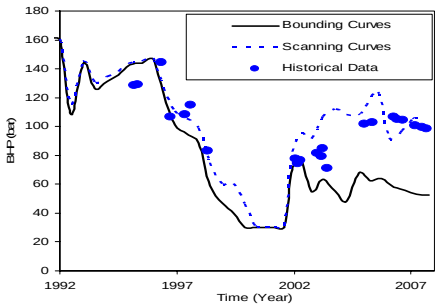

Figure 9a: History match of measured down hole pressure (symbols) using two relative permeability models 1- bounding curves alone (solid line) and 2- scanning curves (dashed line).

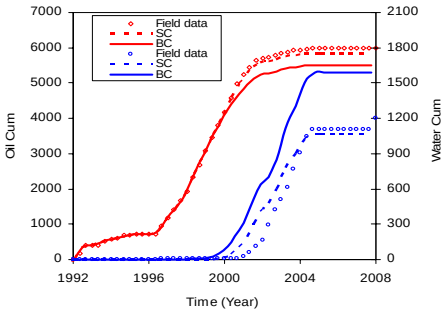

Figure 9b: History match of oil and water cumulative production of a crestal well using two relative permeability models 1- bounding curves alone (BC -solid lines) and 2- scanning curves (SC-dashed lines).

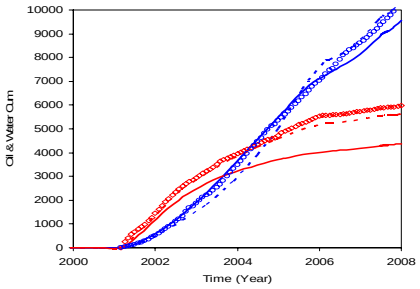

Figure 10: History match of oil and water cumulative production of a flank well (A) using two relative permeability models 1- bounding curves alone (solid lines) and 2- scanning curves (dashed lines).